Volume 16, Issue 3, 162521 (1-10)

International Journal of Nano Dimension (IJND)

https://dx.doi.org/10.57647/j.ijnd.2025.1603.21

Design and simulation of concentrator plasmonic nanostructure optical antenna to improve the performance of Li-Fi communication technology

Shabnam Andalibi Miandoab[1,*], Sarbast Saleem Hars[2]

[1]*Department of Electrical Engineering, Tabriz Branch, Islamic Azad University, Tabriz, Iran.*
[2]*Industrial Nanotechnology Research Center, Tabriz Branch, Islamic Azad University, Tabriz, Iran.*

[*]**Corresponding author:** sh.andalibi@iaut.ac.ir

Original Research

Received:
1 September 2024
Revised:
10 January 2025
Accepted:
17 January 2025
Published online:
1 June 2025

Abstract:

The use of Li-Fi for the next generations of Internet of Things (IoT) and 6G networks can be very effective. Optical antennas (OAs) can generate a greater optical gain and a wider field of view (FoV). Therefore, they are very efficient in visible light communication (VLC). In this paper, we have studied a concentrator plasmonic nanostructured optical antenna that works in the visible wavelength. For this purpose, the impact of the shape and size of the plasmonic nanostructure was explored to enhance gain and improve the focusing of the optical antenna toward the detector's small surface. To increase the gain and improve the performance of the antenna, periodic nanostructures of comb teeth with varying sharpness and slope have been employed. The plasmonic nanostructures near the luminescent dielectric layer have formed a powerful electromagnetic field resonator and have increased the power up to three times in the optimal state. Moreover, the newly implemented optimal design has demonstrated an expanded FoV range. Consequently, this optical antenna has created a high data transmission rate by increasing the light cocentration.

Keywords: Internet of Things (IoT); Li-Fi technology; Luminescent organic semiconductors; Optical nanoantennas; Surface plasmonic resonance

1. Introduction

Visible light communication (VLC) provides an emerging field of study and research for the use of optical communication and telecommunication (Li-Fi) as a complement to Wi-Fi wireless communication [1–3]. This technology can significantly enhance available bandwidth, thus enabling the transfer of high data rates. Research in the field of novel sciences has always been of special importance [4–8]. With the advancements in long-term internet services like IoT, pervasive networks, smart cities, health facility communication, autonomous vehicles, industrial machine communication, augmented reality, and Intelligent Transportation Systems (ITS), the demand for utilizing additional electromagnetic bands has increased compared to previous times[9–11]. Therefore, due to the high traffic of the radio frequency (RF), the next generation of wireless communications such as 6G can fully use the licensed exempt optical spectrum range to send data. For this purpose, the environment illumination light is used. So the information for transmission is placed on it in a modulated form. Intensity modulation of LED light sources is possible with high speed [12–15]. Therefore, internal lighting or external illumination sources can easily be effective for transmitting the required data in next-generation IoT devices [16]. The actual performance of optical communication is formed in the Li-Fi network structure, which will have a high potential for providing long-range wireless communication in the future smart world. One of the important challenges for the development of this technology is the design of an ideal receiver of the type of optical antennas for it. A suitable receiver has low-cost manufacturing technology and can provide high optical gain, high sensitivity, high operating speed, and a large field of view (FoV) [17, 18]. One approach to increase the sensitivity of VLC receptors is to increase the photon receiving level for the detector [19, 20]. While in this situation, the cost of production will increase and at the same time the performance speed will decrease. An effective strategy involves employing passive optical components to

concentrate the light, although this may limit the FoV in the receiver. On the other hand, the optical nanoantennas of the luminescence concentrator structure in the visible light range can free the VLC detectors from complex tracking systems and turn them into a suitable structure for use in smart terminals with simple methods [21–24]. They are able to convert the incident photons to longer wavelengths with good quantum efficiency and transfer the generated wavelengths from a large receiving area to a small photo diode (PD) surface for high-speed detection. Surface plasmonic resonance is a key factor in the research of optical nanoantennas. Metal nanostructures significantly enhance surface plasmon resonance in the visible light spectrum for electromagnetic waves by increasing the metal-dielectric boundary surface [25–28]. In this way, they play an effective role in controlling the direction and increasing the optical gain of this type of antenna. One of the objectives of this study is to provide a relatively complete simulated structure with adequate accuracy for the study of the fundamental parameters of nanostructured optical antennas. So that by eliminating the costs and complexities of experimental work, the effect of structural parameters can be studied and a correct prediction of the performance of the proposed technologies can be provided. For this purpose, in this article, we have designed and simulated an initial structure of a nanostructured optical antenna concentrating luminescence based on the surface plasmonic effect. We have initially validated our simulations by comparing them to experimental data from reputable sources to ensure the correctness and accuracy of the performed calculations, and then we have studied and optimized the structure. To increase the efficiency and improve the gain of the concentrator antenna, we have utilized the help of periodic nanostructures, and we have investigated the effect of the parameters and dimensions of the nanostructure on the basic characteristics of the concentrator antenna. Considering that the comb tooth nanostructures used are made of Ag metal, by using the characteristics of surface plasmon resonance, they play a great role in increasing the efficiency of the optical antenna in the visible wavelength spectrum. The effect of the dimensional characteristics of these plasmonic nanostructures on the basic parameters of the intended antenna has been completely studied in this article. Thus, in this article we have shown that nanostructure optical antennas (OAs) can generate a greater optical gain and the shape and size of the plasmonic nanostructure significantly influence the performance of them. Then with optimizing the plasmonic nanostructures in our suggested structure we have formed a powerful electromagnetic field resonator and have increased the power of radiation light up to three times.

2. Materials and methods

2.1 Calculation method

For simulation, light is considered as an electromagnetic wave, and the method of numerical solution of Maxwell's equations is used to obtain the distribution of fields in different layers of the structure. For this purpose, FDTD Solutions calculation method has been used in 2D to perform optical response calculations and obtain electric field distribution on the designed structure [31]. To investigate the propagation of light waves in different layers of the optical antenna using the FDTD method, Maxwell's equations have been calculated in discrete time using the Finite Difference numerical solution method, and the distribution of electric fields (**E**) and magnetic fields (**H**) in different areas has been obtained using the following equations:

$$\mathbf{E}^{(n+1)} = \mathbf{E}^{n} + \frac{\Delta t}{\varepsilon}\nabla \times \mathbf{H}^{(n+\frac{1}{2})} \tag{1}$$

$$\mathbf{H}^{(n+\frac{3}{2})} = \mathbf{H}^{(n+\frac{1}{2})} - \frac{\Delta t}{\mu}\nabla \times \mathbf{E}^{(n+1)} \tag{2}$$

By obtaining the field distributions, the radiation and reflection components of the optical power have been calculated as:

$$P(\lambda) = \int \frac{1}{2} c\varepsilon_0 n\alpha |E(x,y,z)|^2 dxdydz \tag{3}$$

where c is the speed of light in free space, ε_0 is the permittivity of vacuum, n is the real part of the refractive index, $\alpha = 4\pi k/\lambda$, k is the imaginary part of the refractive index, and E is the electrical field distribution obtained from the FDTD method at different locations.

The simulated structure in the software environment is according to Fig. 1 (a). To simulate the light source as a field distribution with a wide bandwidth in the visible wavelength range of 350 nm − 800 nm under normal radiation to the surface of the structure is considered. In addition, for the structure of the studied nanoantenna with the same periodicity, the source is considered as a flat wave. The propagation direction is assumed to be perpendicular to the surface of the structure (reverse direction of the y axis), where the calculations are done in the x-z plane. For simulation, only one periodicity of $\Lambda = 500$ nm is modeled, and in the existing boundaries along the x direction, the boundary conditions are periodic. PML (Perfectly match layer) boundary conditions are considered along the y direction. The size of the mesh cells used for the specified simulation area is considered to be about 0.2 nm to have a high accuracy of the calculations according to the used structure.

2.2 Flat structure of thin film concentrator optical antenna

The under study planar structure, in three-dimensional form and the arrangement of the layers as seen from the front, as well as the simulated structure of the thin film antenna in the software environment, have been shown in Fig. 1 (b). The structure considered for concentrator antenna utilizes a compound parabolic structure (CPC) (Fig. 1 (c)). Light is irradiated to the surface of the structure in the inverse y direction. According to the fact that the side edges and the bottom have a mirror state and the structure of the antenna is made of transparent layers with a slight difference in refractive index, the light is concentrated inside the structure and is directed towards the output in the x direction. Due to the photoluminescence feature of the layers, the absorbed light radiates with a wavelength shift towards larger wavelengths at the output. The arrangement of the layers and their thickness next to each other for the structure in a period (Λ) is shown as a view from the front (x-y) in Fig. 1 (c).

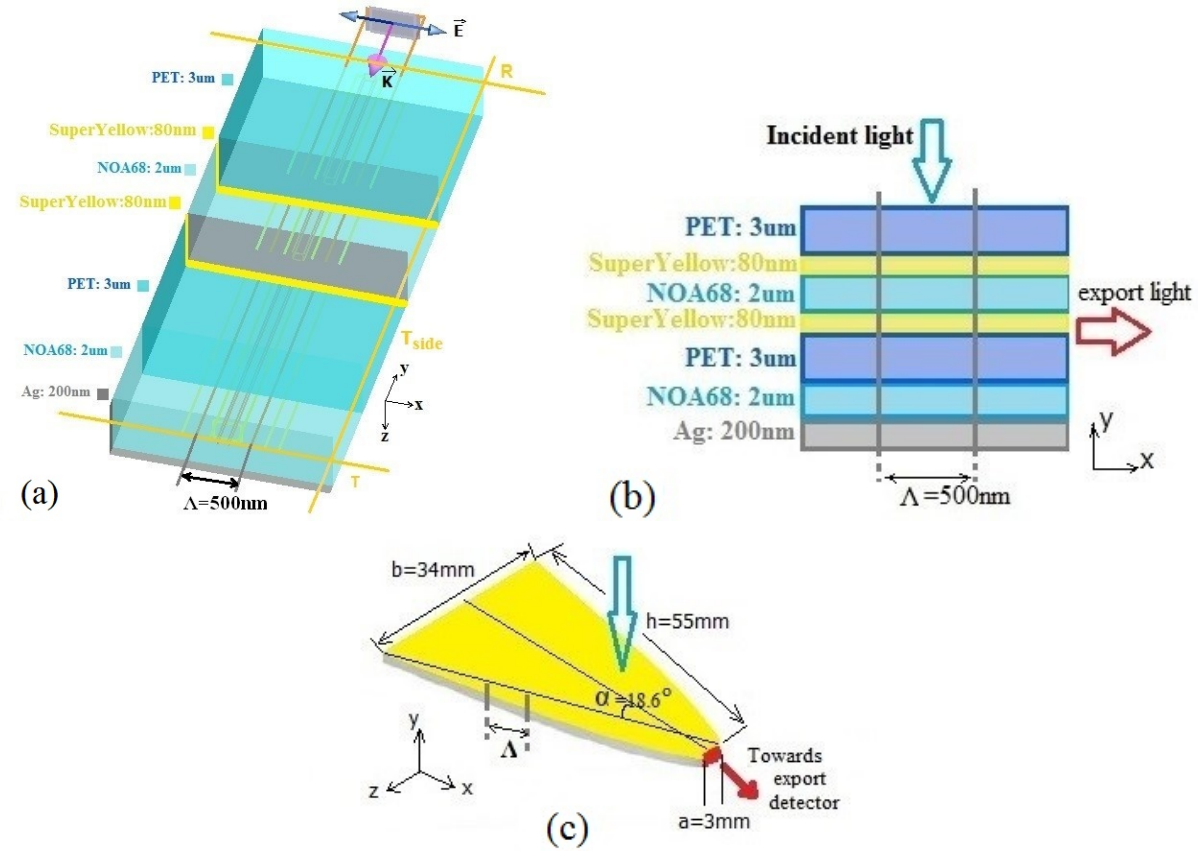

Figure 1. (a) Simulated structure in the software environment, (b) Layered structure created in the periodic range as seen from the front, (c) Schematic of CPC luminescence concentrating optical antenna.

As shown, the lowest layer is silver (Ag), which is considered as a reflective layer with a thickness of 200 nm. Two layers of NOA68 with a refractive index of 1.54 and a thickness of 2 μm, which are relatively transparent, along with two layers of Super Yellow with a thickness of 80 nm, which are actually composed of Ph-ppv molecules and have photoluminescence properties, have been used to increase the dominant light density. The molecular structure and optical properties used to simulate this layer are illustrated in Figs. 2 (a), 2 (b) [29, 30]. Two layers of PET with a refractive index of 1.575 and a thickness of 3 μm have been used, one as a substrate and the other to help collect light in the waveguide structure in the displayed locations.

2.3 The structure of a thin film concentrator optical antenna with a layer containing comb nanoteeth

To study and increase the performance of focusing optical antenna, we use comb tooth nanostructures in thin film layering. The studied structure in three dimensions and the arrangement of the layers as a front view as well as the simulated structure of the thin film antenna in the software environment are shown in Figs. 3 (a), 3 (b). The general structure considered for the concentrating optical antenna in this case is also in the form of compound parabolic concentrator (CPC) (Fig. 1 (c)). Light is irradiated to the surface of the structure in the inverse y direction. Considering that the side edges and the bottom have a mirror state and the

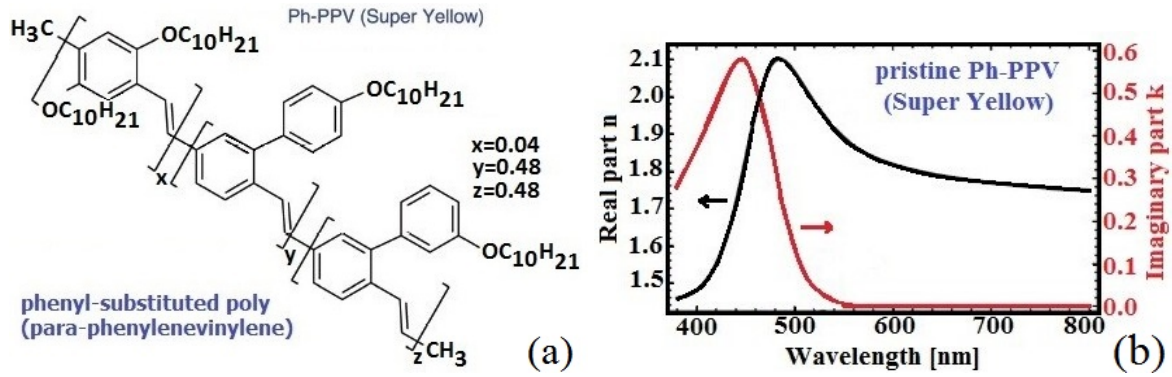

Figure 2. (a) Molecular structure of Ph-ppv layer as SuperYellow layer, (b) Optical characteristic in the form of real and imaginary refractive index for Ph-ppv polymer layer [29, 30].

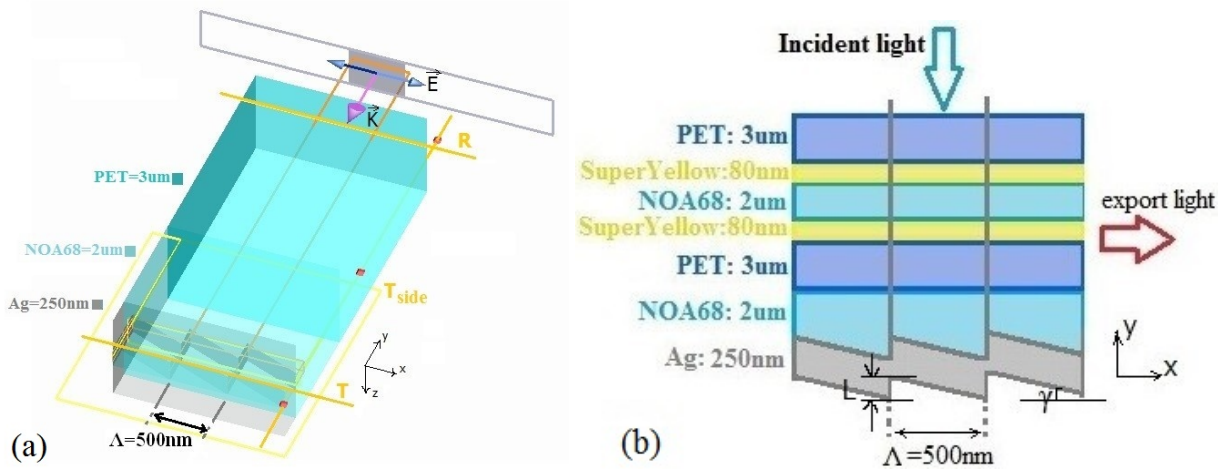

Figure 3. (a) The simulated structure in the software environment for the concentrator with comb tooth nanostructures, front view (value of the period of the structure $\Lambda = 500$ nm and the inclination angle of the teeth γ), (b) Schematic of the concentrator of comb tooth nanostructures created in the form of a layered structure.

structure of the antenna consists of transparent layers with a slight difference in refractive index, the light is trapped inside the waveguide area. Nano-structures of metal comb tooth have been used to enhance surface plasmonics properties, leading to increased field intensity and concentration in the waveguide layers.

Finally, the focused light is guided towards the exit along the x-axis. In this way, we have improved the performance of concentrating antennas with nanostructures. Due to the photoluminescence property of the layers, the absorbed light radiates with a wavelength shift towards larger wavelengths at the output. The arrangement of the layers and their thickness next to each other as seen from the front (x-y plane) is shown in Fig. 3 (b). As seen in Fig. 3 (b), the lowest layer, which is composed of Ag metal, has created nanoscale comb tooth structures. The NOA68 layer's excellent patterning capability allows for precise nano gratings creation, facilitating the study of fundamental characteristics of the concentrating antenna by modifying the structure's components. According to the established structure, the periodicity considered for this periodic structure is $\Lambda = 500$ nm, which is assumed to be constant. Then, by changing the height of the created teeth, which leads to the change of the γ angle and the change of the sharpness of the teeth, we study the effect of surface plasmonics on the concentration of the electromagnetic field.

The optical gain characteristic for a nanostructured optical antenna can be calculated from the equation, $OG = \frac{A_{\text{in}}}{A_{\text{out}}}\eta$, where A_{in} is the total area of the antenna for incident light and A_{out} is the area of the light transmission area towards the detector. The ratio of these two surfaces creates the geometrical gain that can be calculated according to the structural specifications of the CRC antenna (α, b, h, and a) as shown in Fig. 1 (c). On the other hand, the total optical efficiency is obtained from the equation, $\eta = \frac{P_{\text{out}}}{P_{\text{in}}}$. Considering that in both the flat and comb nanoteeth structures studied in this article, the areas of A_{in} and A_{out} are assumed to be constant, and the input light power (P_{in}) to both structures is the same. The parameter that has been used as the main component of optical gain in this study to analyze and compare the results is the output optical power (P_{out}).

3. Results and discussions

3.1 Absorption and side radiation spectrum of flat structure optical antenna

The absorption and emission spectra calculated for the simulated structure according to Fig. 1 (a) compared to the experimental results presented in reference [32] are given in Figs. 4 (a), 4 (b), 4 (c). As can be seen, absorption and emission spectrums are created in the visible light range. The absorption spectrum has a peak around the 430 nm wavelength and the luminescence emission spectrum has a peak around the 540 nm wavelength. The exact value of the resonance wavelength for the absorption and side radiation spectrum resulting from the calculations performed in this article compared to the experimental results presented in the valid reference is given in Table 1 [32]. According to the results, the resonance wavelength in the photoluminescence side radiation spectrum shows a shift towards longer wavelengths. According to Fig. 1 (b), the structure of the antenna in question consists of various layers that actually create the structure of a dielectric waveguide for the incidence electromagnetic light. Each of these layers is defined in the simulation environment by its optical properties, which actually determine the appearance of their dielectric coefficient in the desired wavelength range. In this way, the calculations performed and the distributions of the overall fields obtained for the structure, have been analyzed the losses, and scatterings present in all layers.

Then for further study, the concentrator antenna with a flat structure has been considered (Fig. 5 (a)) and by changing the radiation angles of the electromagnetic field applied in the space around it. The obtained results compared to each other are displayed next to the desired structure in Fig. 5. The field concentration (Fig. 5 (b)), the radiation (Fig. 5 (c)) and reflection pattern (Fig. 5 (d)) is calculated so that by changing the structure, we can provide a more suitable pattern. One of the essential characteristics of an antenna can be its FOV. To demonstrate this ability of the

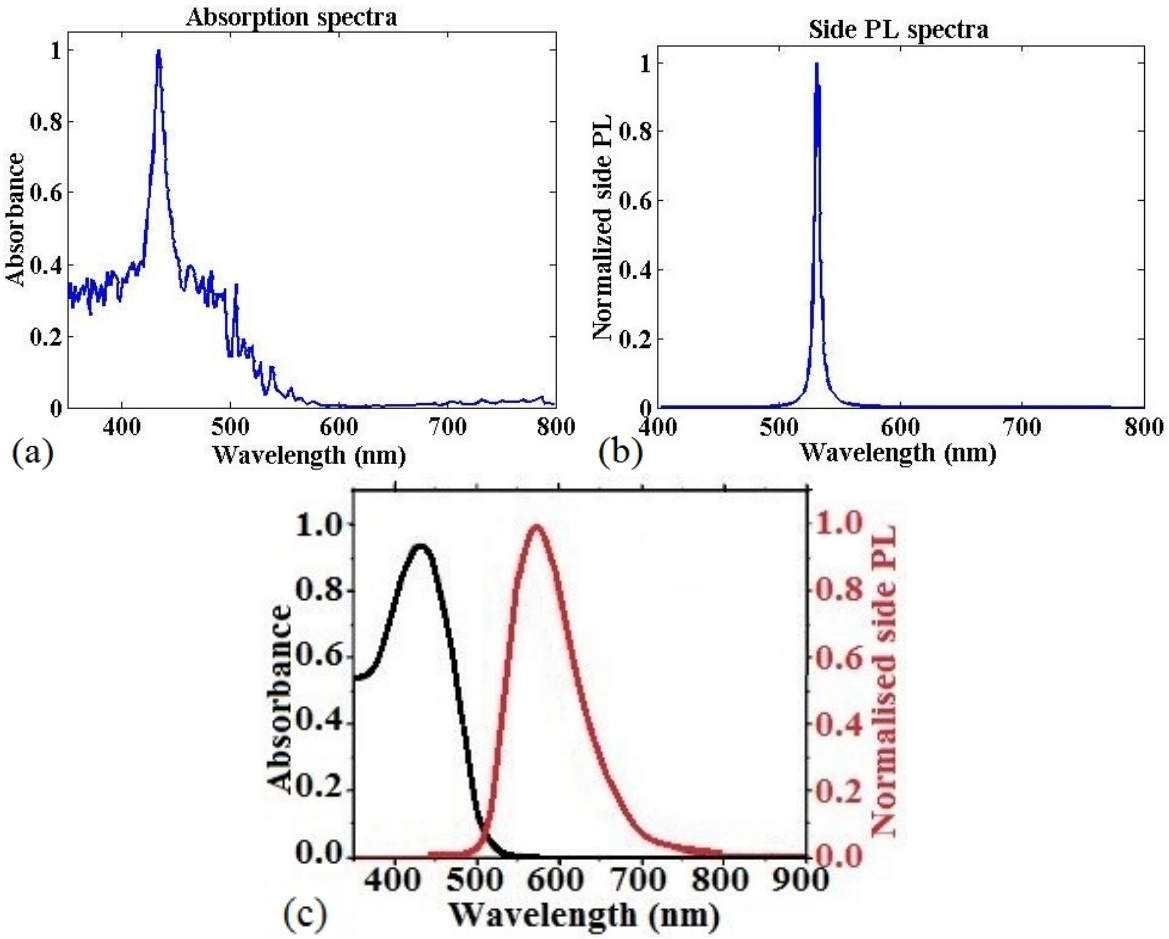

Figure 4. (a) Calculated absorption spectrum of the flat concentrator antenna, (b) Calculated photoluminescence side radiation spectrum of the flat concentrator antenna, (c) Absorption and side radiation spectrum of the concentrator antenna experimentally [32].

desired antenna to receive information, we have used the radiation pattern to make a proper evaluation of its performance in collecting information from surrounding environment, and create another comparative criterion between the proposed structures. According to the results of Fig. 5 (c), the radiation pattern that demonstrates the ability to receive electromagnetic fields by the flat antenna is positioned at the zero-degree incidence angle in the outer radius and generating greater reception power, this amount decreases as the incidence angle increases. Since the changes in radiation efficiency for different receiving angles are small, it can be said that the antenna has a good FOV. However given the small amount of radiation efficiency (which is maximally around 0.5), we have tried to improve this amount in the proposed structure. The radiation field distribution has also been obtained for this structure. As can be seen in Fig. 5 (b), the field concentration in the waveguide region causes the concentration and transfer of light towards the detector. As shown in Fig. 1 (c), to have accurate studies with small mesh size that can fully investigate the consideration nanostructure and its interactions with the around environment, The simulations have been performed in a period (Λ) of the structure and the results have been obtained for a unit cell of the structure with dimensions of the considered period.

3.2 Absorption and side radiation spectrum of comb tooth nanostructure optical antenna

For the concentrator antenna with comb tooth grating nanostructures with the same periodicity, the source is considered as a flat wave. For simulation only one periodicity of $\Lambda = 500$ nm is modeled and periodic boundary conditions are applied in the boundaries created in the x direction. In

Table 1. Resonance wavelength for absorption and side radiation spectrum for the experimental sample compared to the simulated model.

Sample of a concentrator antenna	Experimental sample [32]	Computational simulation model in this study
Resonance wavelength of absorption spectrum	433 nm	434 nm
Resonance wavelength of side radiation spectrum	545 nm	534 nm

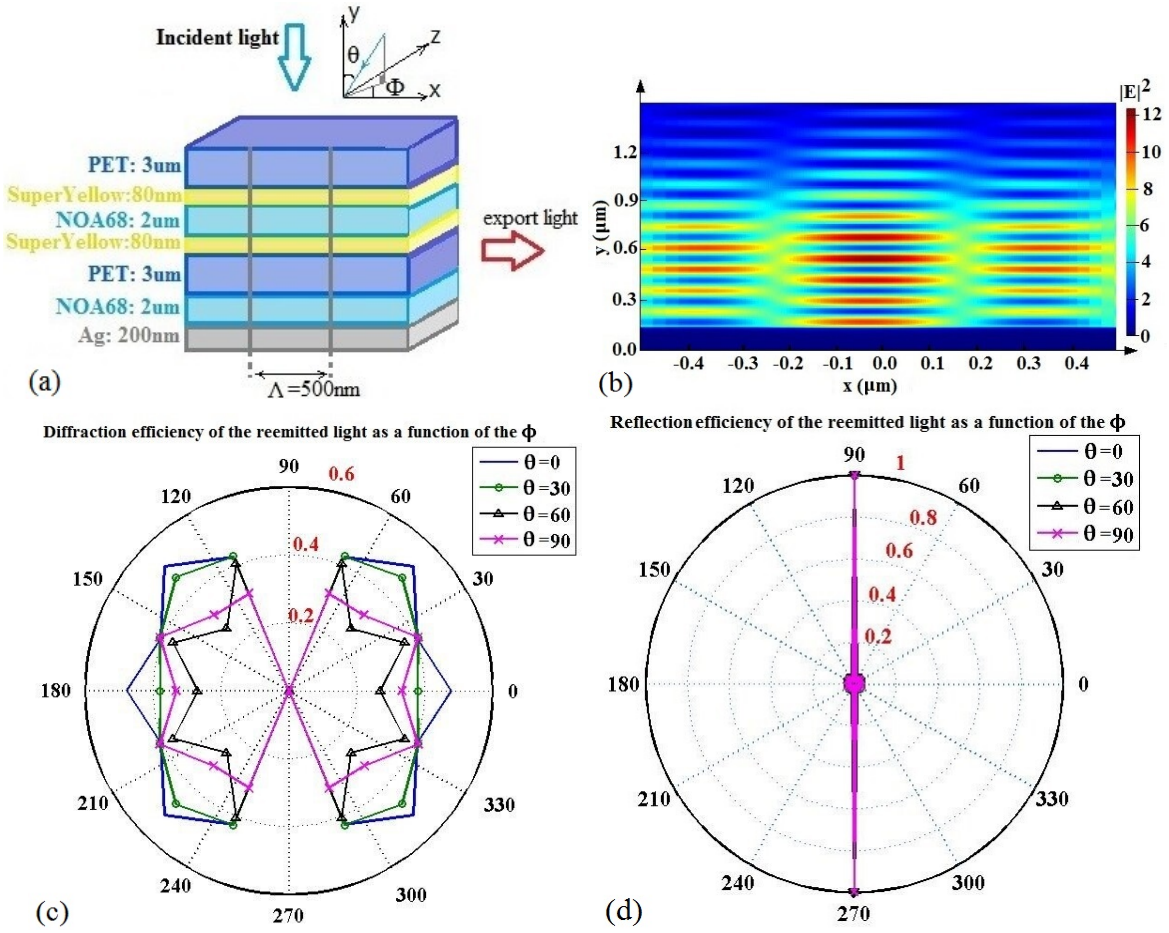

Figure 5. (a) The structure of the concentrator antenna by changing the desired radiation angles, (b) The distribution of the radiation field near the waveguide surface of the flat structure of the concentrator antenna, (c) The radiation pattern of the far field by changing the angle Φ for different values of the angle θ for Two-way space antenna, (d) Far-field reflection pattern with change of angle Φ for different values of angle θ for two-way space antenna.

the y-direction, where there is no periodic structure, Perfectly Matched Layer (PML) conditions are assumed. The considered structure is shown in figure 3. The radiation spectrum calculated for the Ag plasmonic comb tooth grating structures for variable tooth slope angle $\gamma = 11°$, 17°, 22°, 27°, 31°, 35° corresponding to the height of the teeth $L = 100$ nm, 150 nm, 200 nm, 250 nm, 300 nm and 350 nm with periodicity $\Lambda = 500$ nm are shown in Figs. 6 (a)-6 (f), respectively. As seen, the peak intensity of the created resonance wavelength varies according to the geometrical change of the structure. To some extent, increasing the angle of the teeth due to the increase in the surface area, the surface plasmonic intensity is increasing, so the intensity of the radiation spectrum also increases. However, more than a certain limit, with the decrease in wave guide power due to the inhibition of the teeth, the plasmonic intensity and consequently the intensity of radiation spectrum decrease. To show how the peak intensity of the field (the field at the resonant wavelength $\lambda = 530$ nm) changes in relation to the changes in the slope angle of the teeth of the nanostructure, we have drawn the calculated values in Fig. 7. As can be seen, the intensity of the field increases up to the angle $\gamma = 31°$, while after that the intensity of the field decreases with the decrease of the concentration level.

In continuation, to further study the concentrator optical antenna with plasmonic effects in surface-grating nanostructures (Fig. 8 (a)) and the changes in angles of electromagnetic field radiation have been considered. The obtained results compared to each other are displayed next to the desired structure in Fig. 8. The field concentration (Fig. 8 (b)), the radiation (Fig. 8 (c)) and reflection patterns (Fig. 8 (d)) in the space around it have been calculated. From the comparison of the results with the concentrating antenna of the flat structure, it can be seen that the antenna created with the grating nanostructure creates a greater field concentration (Figs. 8 (c), 8 (d)). Also, a stronger radiation field has been created around the plasmonic nanostructures in an intensified form, which has made it more appropriate to guide the detector towards the detector according to the inclination of the teeth (Fig. 8 (b)). In this way, by increasing the concentration, a large optical gain is created and a receiver with suitable characteristics is created. Considering that in order to have accurate results in the nanostructure dimensions, calculations have been performed in one period (Λ) of the structure, the results examined in Fig. 8 are also shown in the dimensions considered for simulation.

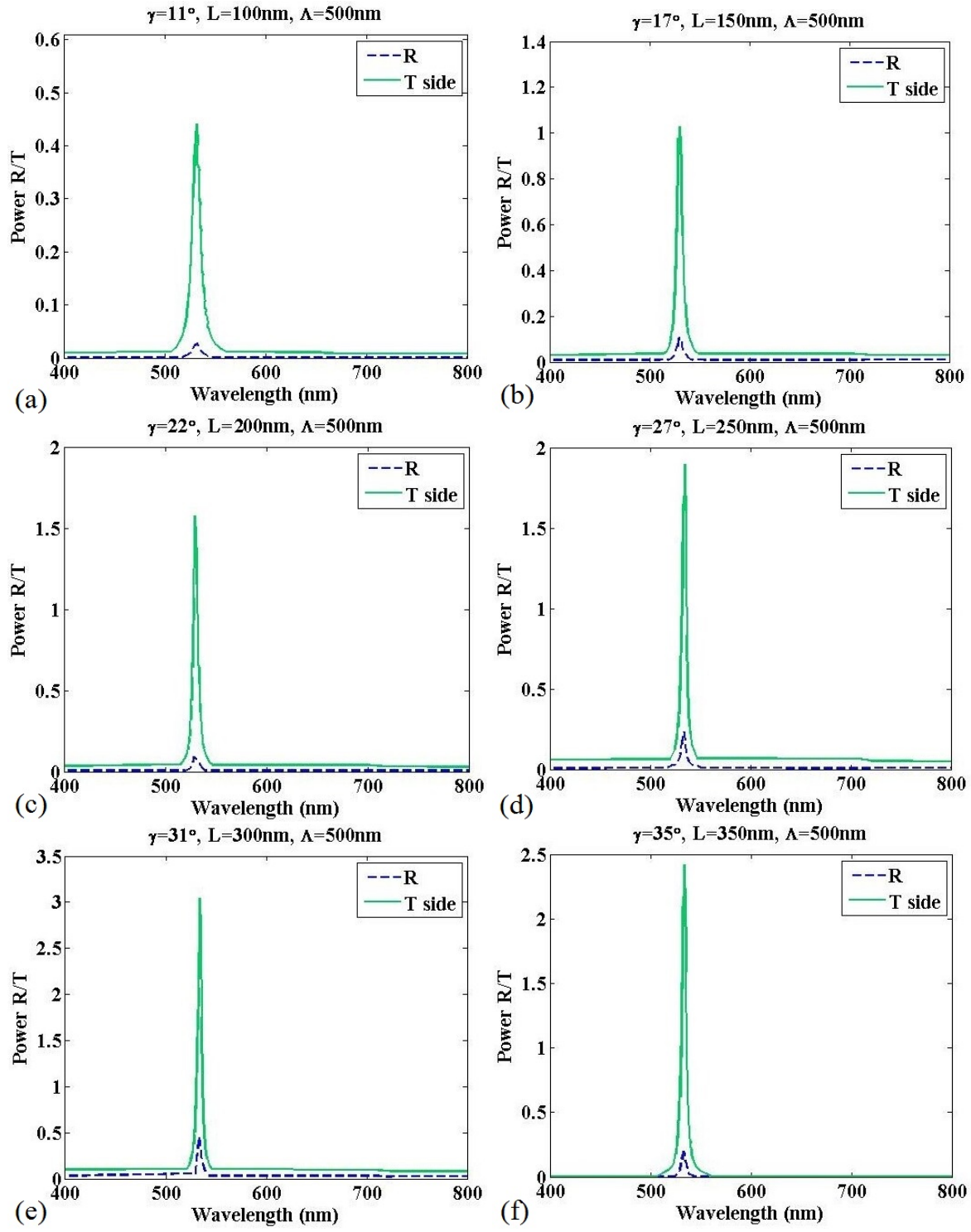

Figure 6. The calculated radiation spectrum of the concentrator antenna with comb tooth nanostructures for different geometric characteristics (a) $L = 100$nm, $\Lambda = 500$nm, $\gamma = 11°$, (b) $L = 150$nm, $\Lambda = 500$nm, $\gamma = 17°$, (c) $L = 200$nm, $\Lambda = 500$nm, $\gamma = 22°$, (d) $L = 250$nm, $\Lambda = 500$nm, $\gamma = 27°$, (e) $L = 300$nm, $\Lambda = 500$nm, $\gamma = 31°$, (f) $L = 350$nm, $\Lambda = 500$nm, $\gamma = 33°$.

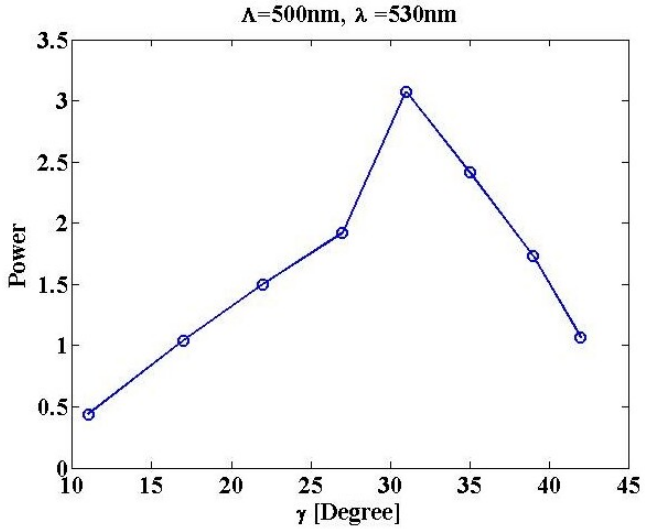

Figure 7. Variations of field peak intensity (field at resonant wavelength $\lambda = 530$nm) in relation to variations of the slope angle of nanostructure teeth in the grating concentrator antenna with plasmonic effect.

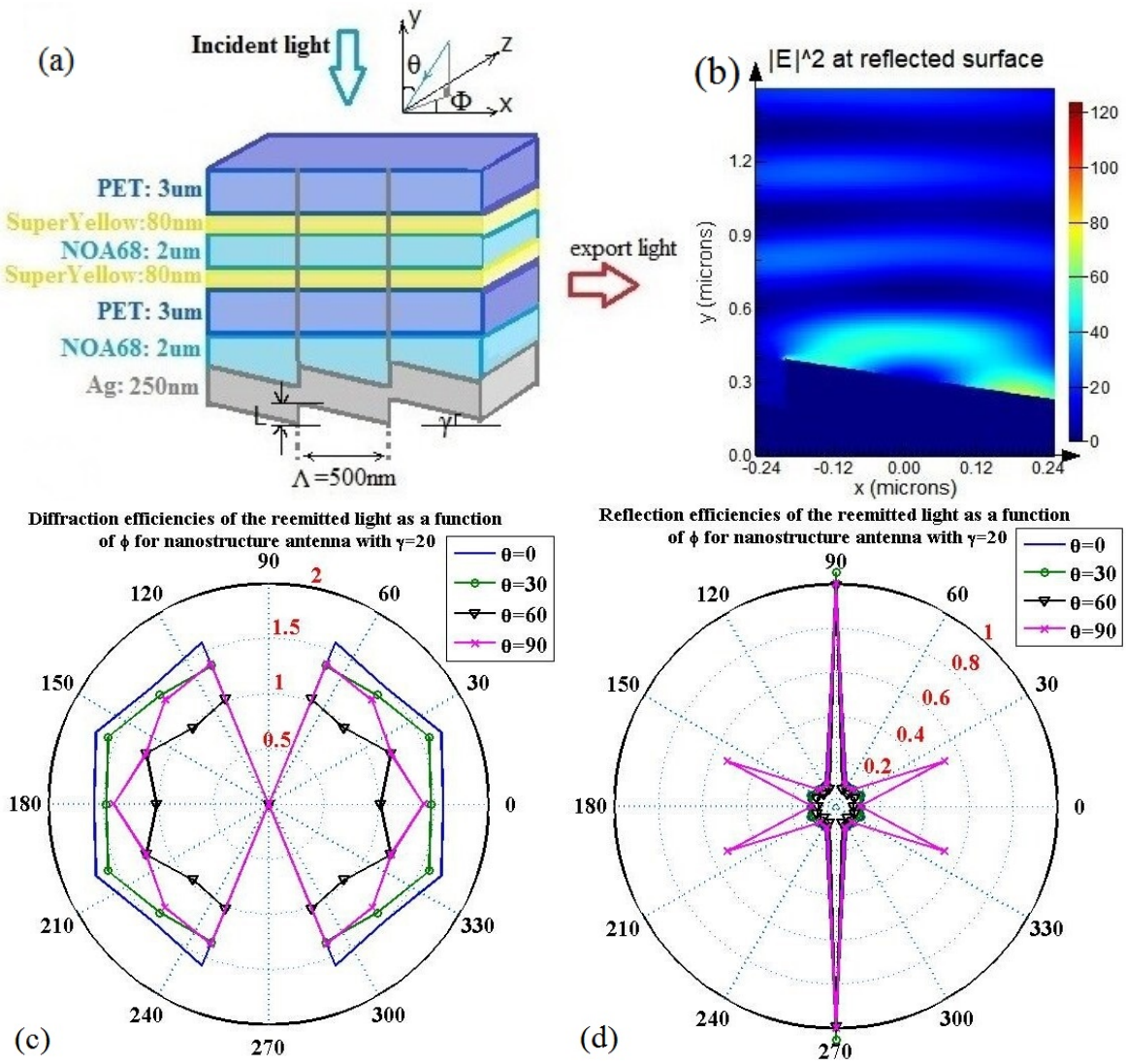

Figure 8. (a) The structure of the concentrator antenna with grating nanostructures by changing the desired radiation angles, (b) The radiation field distribution near the surface of the grating nanostructures with surface plasmonic effect, (c) The far-field radiation pattern by angle changing Φ for different values of angle θ for the bidirectional spatial concentrator antenna with grating nanostructures, (d) far-field reflection pattern with angle change Φ for different values of angle θ for the bidirectional spatial concentrator antenna with grating nanostructures.

4. Conclusion

The studies and research show that data transmission in Li-Fi communication technology is still associated with deficiencies due to the amount and speed of information transfer. Also, despite the advantages that plasmonic optical antennas provide for Li-Fi system receivers, there are still challenges in improving performance and efficiency in optical communications. In this article, we have worked on the design and simulation of fluorescence nanostructure concentrating antennas for Li-Fi communication technology. The approach that we have presented includes an optical antenna structure in the form of flat CPC, and a structure with layers of nano gratings with surface plasmonic effect of suitable shape and size. Due to the fact that based on field studies and review of existing records, most of the practical and experimental reports and articles have been worked in this field we have tried to present a complete simulated model for this purpose. Therefore, for the comparability of the studies, we first created the structure of the thin film concentrator antenna exactly similar to the structures presented in the valid experimental articles and compared the results which were in good agreement with the experimental samples. In this way, after making sure of the correctness and accuracy of the calculations, we have studied, designed and optimized the proposed structure. Numerical methods are of special importance in modeling and simulating the characteristics of optical devices. For this purpose, FDTD numerical methods are used for simulation, which are suitable for designing and simulating optical devices. We have used this method to design the 2D structure of the corresponding optical antenna. In this way, all Maxwell's equations are discretized by using the definition of the derivative and considering the appropriate boundary conditions in the whole structure, it is solved and the distribution of electromagnetic fields is calculated. With this method, first the absorption and concentrated radiation spectrum for the primary structure is calculated, then by placing the layer made of grating nanostructures with the surface plasmonic effect, the created optical spectrum is calculated and the results are compared. Then, with changes in the geometric characteristics of the layer formed by the grating nanostructures, which included variations in the sharpness of slope and height of the comb teeth, we studied the field intensity and the spectral concentration of the antenna and introduced the optimal structure. Therefore, a large part of the light can be collected by the introduced optical antenna and detected by the optical detector placed on the limited surface.

Authors contributions
Authors have contributed equally in preparing and writing the manuscript.

Availability of data and materials
The authors declare that the data supporting the findings of this study are available within the paper.

Conflict of interests
The authors assert that they do not have any identifiable conflicting financial interests or personal relationships that might be perceived to influence the work presented in this paper.

References

[1] V. Jungnickel, M. Hinrichs, K. Bober, C. Kottke, A. Corici, M. Emmelmann, J. Rufo, P. B. Bök, D. Behnke, and M. Riege. "Enhance lighting for the internet of things.". *2019 Global LIFI Congress (GLC)*, 2019.

[2] H. Haas, L. Yin, Y. Wang, and C. Chen. "What is lifi?". *Journal of Lightwave Technology*, 34(6):1533–1544, 2015. DOI: https://doi.org/10.1109/JLT.2015.2510021.

[3] S. Alfattani. "Review of LiFi technology and its future applications.". *Journal of Optical Communications*, 42(1):121–132, 2021. DOI: https://doi.org/10.1515/joc-2018-0025.

[4] M. S. Sadjadi, B. Sadeghi, and K. Zare. "Natural bond orbital (NBO) population analysis of cyclic thionylphosphazenes, [NSOX (NPCl2)2]; X = F (1), X = Cl (2).". *Journal of Molecular Structure: THEOCHEM*, 817:27–33, 2007. DOI: https://doi.org/10.1016/j.theochem.2007.04.015.

[5] M. Sadjadi, M. Meskinfam, B. Sadeghi, H. Jazdarreh, and K. Zare. "In situ biomimetic synthesis and characterization of nano hydroxyapatite in gelatin matrix.". *Journal of Biomedical Nanotechnology*, 7: 450–454, 2011. DOI: https://doi.org/10.1166/jbn.2011.1305.

[6] B. Sadeghi, S. Ghammamy, Z. Gholipour, M. Ghorchibeigy, and A. A. Nia. "Gold/hydroxypropyl cellulose hybrid nanocomposite constructed with more complete coverage of gold nano-shell.". *Micro & Nano Letters*, 6:209–213, 2011. DOI: https://doi.org/10.1049/mnl.2011.0036.

[7] A. Amininia, K. Pourshamsian, and B. Sadeghi. "Nano-ZnO impregnated on starch—A highly efficient heterogeneous bio-based catalyst for one-pot synthesis of pyranopyrimidinone and xanthene derivatives as potential antibacterial agents.". *Russian Journal of Organic Chemistry*, 56:1279–1288, 2020. DOI: https://doi.org/10.1134/S1070428020070234.

[8] B. Sadeghy and S. Ghammami. "Oxidation of alcohols with tetramethylammonium fluorochromate in acetic acid.". *Russian Journal of General Chemistry*, 75:1886–1888, 2005. DOI: https://doi.org/10.1007/s11176-006-0008-0.

[9] N. Chen and M. Okada. "Toward 6G internet of things and the convergence with RoF system.". *IEEE Internet of Things Journal*, 8 (11):8719–8733, 2020. DOI: https://doi.org/10.1109/JIOT.2020.3047613.

[10] A. Gohar and G. Nencioni. "The role of 5G technologies in a smart city: The case for intelligent transportation system.". *Sustainability*, 13(9):5188, 2021. DOI: https://doi.org/10.3390/su13095188.

[11] D. Tsonev, S. Videv, and H. Haas. "Light fidelity (Li-Fi): towards all-optical networking.". *Broadband Access Communication Technologies VIII*, 9007:900702, 2014. DOI: https://doi.org/10.1117/12.2044649.

[12] L. Grobe, A. Paraskevopoulos, J. Hilt, D. Schulz, F. Lassak, F. Hartlieb, C. Kottke, V. Jungnickel, and K.-D. Langer. "High-speed visible light communication systems.". *IEEE Communications Magazine*, 51(12):60–66, 2013.
DOI: https://doi.org/10.1109/MCOM.2013.6685758.

[13] X. You, C.-X. Wang, J. Huang, X. Gao, Z. Zhang, M. Wang, Y. Huang, C. Zhang, Y. Jiang, and J. Wang. "Towards 6G wireless communication networks: Vision, enabling technologies, and new paradigm shifts.". *Science China Information Sciences*, 64:1–74, 2021.
DOI: https://doi.org/10.1007/s11432-020-2955-6.

[14] P. P. Manousiadis, H. Chun, S. Rajbhandari, D. A. Vithanage, R. Mulyawan, G. Faulkner, H. Haas, D. C. O'Brien, S. Collins, and G. A. Turnbull. "Optical antennas for wavelength division multiplexing in visible light communications beyond the étendue limit.". *Advanced Optical Materials*, 8(4):1901139, 2020.
DOI: https://doi.org/10.1002/adom.201901139.

[15] R. Mulyawan, A. Gomez, H. Chun, S. Rajbhandari, P. P. Manousiadis, D. A. Vithanage, G. Faulkner, G. Turnbull, I. D. Samuel, and S. Collins. "A comparative study of optical concentrators for visible light communications.". *Broadband Access Communication Technologies XI*, 10128:142–147, 2017.
DOI: https://doi.org/10.1117/12.2252355.

[16] M. Meucci, S. Doria, A. M. Umair, D. Franchi, M. Fattori, M. Di Donato, A. Picchi, A. Pucci, M. Calamante, and J. Catani. "Efficient White-Light Visible Light Communication With Novel Optical Antennas Based on Luminescent Solar Concentrators.". *Journal of Lightwave Technology*, 42(7):2235–2244, 2023.
DOI: https://doi.org/10.1109/JLT.2023.3337040.

[17] P. P. Manousiadis, S. Rajbhandari, R. Mulyawan, D. A. Vithanage, H. Chun, G. Faulkner, D. C. O'Brien, G. A. Turnbull, S. Collins, and I. D. Samuel. "Wide field-of-view fluorescent antenna for visible light communications beyond the étendue limit.". *Optica*, 3(7):702–706, 2016.
DOI: https://doi.org/10.1364/OPTICA.3.000702.

[18] X. Yang, Y. Dong, P. Zeng, Y. Yu, Y. Xie, J. Gong, M. Shi, R. Liang, Q. Ou, and N. Chi. "Nanopatterned organic semiconductors for visible light communications.". *Young Scientists Forum SPIE*, 10710: 170–175, 2018.
DOI: https://doi.org/10.1117/12.2314698.

[19] R. Carvalho, R. Brito-Pereira, N. Pereira, A. Lima, C. Ribeiro, V. Correia, S. Lanceros-Mendez, and P. Martins. "Improving the performance of paper-based dipole antennas by electromagnetic flux concentration.". *ACS Applied Materials & Interfaces*, 15(8):11234–11243, 2023.
DOI: https://doi.org/10.1021/acsami.2c19889.

[20] H. Ibili, T. Blatter, M. Baumann, L. Kulmer, B. Vukovic, J. Smajic, and J. Leuthold. "Modeling plasmonic antennas for the millimeter-wave & THz range.". *IEEE Journal of Selected Topics in Quantum Electronics*, 2023.
DOI: https://doi.org/10.1109/JSTQE.2023.3314696.

[21] I. Sychugov. "Analytical description of a luminescent solar concentrator.". *Optica*, 6(8):1046–1049, 2019.
DOI: https://doi.org/10.1364/OPTICA.6.001046.

[22] J. Wang, Y. Yuan, H. Zhu, T. Cai, Y. Fang, and O. Chen. "Three-dimensional macroporous photonic crystal enhanced photon collection for quantum dot-based luminescent solar concentrator.". *Nano Energy*, 67:104217, 2020.
DOI: https://doi.org/10.1016/j.nanoen.2019.104217.

[23] M. K. Assadi, H. Hanaei, N. M. Mohamed, R. Saidur, S. Bakhoda, R. Bashiri, and M. Moayedfar. "Enhancing the efficiency of luminescent solar concentrators (LSCs).". *Applied Physics A*, 122:1–12, 2016.
DOI: https://doi.org/10.1007/s00339-016-0359-2.

[24] S. W. Schmitt, G. Sarau, and S. Christiansen. "Observation of strongly enhanced photoluminescence from inverted cone-shaped silicon nanostructures.". *Scientific Reports*, 5(1):17089, 2015.
DOI: https://doi.org/10.1038/srep17089.

[25] C. Tummeltshammer, M. S. Brown, A. Taylor, A. J. Kenyon, and I. Papakonstantinou. "Efficiency and loss mechanisms of plasmonic luminescent solar concentrators.". *Optics Express*, 21(105):A735–A749, 2013.
DOI: https://doi.org/10.1364/OE.21.00A735.

[26] Y. Salamin, W. Heni, C. Haffner, Y. Fedoryshyn, C. Hoessbacher, R. Bonjour, M. Zahner, D. Hillerkuss, P. Leuchtmann, and D. L. Elder. "Direct conversion of free space millimeter waves to optical domain by plasmonic modulator antenna.". *Nano Letters*, 15(12): 8342–8346, 2015.
DOI: https://doi.org/10.1021/acs.nanolett.5b04025.

[27] E. Parcham and S. A. Miandoab. "Introducing nanostructure patterns for performance enhancement in PbS colloidal quantum dot solar cells.". *International Journal of Nano Dimension*, 11(1):18–25, 2020.
DOI: https://doi.org/10.1001.1.20088868.2020.11.1.3.1.

[28] A. Rostami, S. Andalibi, S. Seyyedi, and S. Zabihi. "Enhanced optical absorption in organic solar cells using metal nano particles.". *International Journal of Nano Dimension*, 2013.
DOI: https://doi.org/10.7508/ijnd.2013.02.011.

[29] M. T. Sajjad, P. P. Manousiadis, H. Chun, D. A. Vithanage, S. Rajbhandari, A. L. Kanibolotsky, G. Faulkner, D. O'Brien, P. J. Skabara, and I. D. Samuel. "Novel fast color-converter for visible light communication using a blend of conjugated polymers.". *ACS Photonics*, 2(2):194–199, 2015.
DOI: https://doi.org/10.1021/ph500451y.

[30] T. Lanz, E. M. Lindh, and L. Edman. "On the asymmetric evolution of the optical properties of a conjugated polymer during electrochemical p- and n-type doping.". *Journal of Materials Chemistry C*, 5(19): 4706–4715, 2017.
DOI: https://doi.org/10.1039/C7TC01022B.

[31] S. D. Gedney. "Introduction to the finite-difference time-domain (FDTD) method for electromagnetics.". *Synthesis Lectures on Computational Electromagnetics*, 27, 2011.

[32] Y. Dong, M. Shi, X. Yang, P. Zeng, J. Gong, S. Zheng, M. Zhang, R. Liang, Q. Ou, and N. Chi. "Nanopatterned luminescent concentrators for visible light communications.". *Optics Express*, 25(18): 21926–21934, 2017.
DOI: https://doi.org/10.1364/OE.25.021926.